JOC Article

Chemical Bonding and Structure−Reactivity Correlation in Meldrum's Acid: A Combined Experimental and Theoretical Electron Density Study

Deepak Chopra, Vladimir V. Zhurov, Elizabeth A. Zhurova, and A. Alan Pinkerton*

Department of Chemistry, University of Toledo, Toledo, Ohio 43606

apinker@uoft02.utoledo.edu

Received December 9, 2008

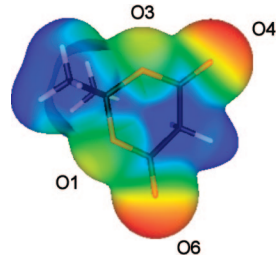

Chemical bonding in Meldrum's acid (MA) based on the experimental electron density obtained from high-resolution X-ray diffraction data at 20 K and from solid state theoretical calculations at the experimental molecular geometry have been analyzed by using the Quantum Theory of Atoms in Molecules. The total electron density was modeled with use of the Hansen−Coppens multipole formalism, and features associated with both intra- and intermolecular bond critical points, topological bond orders, atomic charges, and the electrostatic potential have been characterized and used to understand structure−reactivity relationships. The acidic methylene hydrogen atoms carry modest positive charges. A notable feature is the presence of an intramolecular H···H interaction that imparts stability to the boat conformation. A correlation between the topological bond order and the nature of the chemical bonds in MA illustrates the fact that elimination of carbon dioxide/acetone is an important feature of the chemistry of MA. The surface electrostatic potential and the charge distribution rationalize the sites of nucleophilic/electrophilic attack.

1. Introduction

Meldrum's acid (IUPAC name: 2,2-dimethyl-1,3,-dioxan-4,6-dione, hereafter MA) is a cyclic ester discovered by Meldrum in 1908.[1] The first suggestion that MA had a cyclic bifunctional ester structure was based on chemical intuition and mechanistic insights governing its formation and reactions.[2] This structure was confirmed in 1985 when the first crystal structure analysis of MA was carried out.[3] In addition, this investigation also established the boat form of the six-membered ring, which had been previously postulated based on the measured dipole moment,[4,5] and the presence of C−H···O hydrogen bonds. A striking property of MA is its C−H acidity, with a pK_a value in water in the range of 4.83−4.97.[6] The pK_a measured in DMSO is 7.2,[7] which corresponds well with the value calculated for the gas phase.[8] This acidity is due to the presence of two hydrogen atoms of a methylene group adjacent to two electron-withdrawing carbonyl groups. Spectroscopic measurements, namely IR,[9] UV,[10] and ^{13}C NMR,[11] demonstrate that MA does not undergo enolization, either in solution or in the solid state, to a significant extent.

We note that the removal of the methyl groups from MA, or substitution of one of the methylene hydrogen atoms with an alkyl group, has little influence on the acidity. However, removal

(1) Meldrum, A. N. *J. Chem. Soc.* **1908**, *93*, 598.
(2) Davidson, D.; Bernhard, S. A. *J. Am. Chem. Soc.* **1948**, *70*, 3426.
(3) Pfluger, C. E.; Boyle, P. D. *J. Chem. Soc., Perkin Trans. 2* **1985**, 1547.
(4) Klimovitskii, E. N.; Yuldasheva, L. K.; Arbuzov, B. A. *Izv. Akad. Nauk SSSR, Ser. Khim.* **1973**, 1577.
(5) Köberl, D.; Schuster, P. *Monatsh. Chem.* **1972**, *103*, 1483.
(6) Pihlaja, K.; Seilo, M. *Acta Chem. Scand.* **1969**, *23*, 3003.
(7) Arnett, E. M.; Harrelson, J. A. *J. Am. Chem. Soc.* **1987**, *109*, 809.
(8) Nakamura, S.; Hirao, H.; Ohwada, T. *J. Org. Chem.* **2004**, *69*, 4309.
(9) (a) Eistert, B.; Geiss, F. *Chem. Ber.* **1961**, *94*, 929. (b) Eistert, B.; Geiss, F. *Tetrahedron.* **1959**, *7*, 1. (c) Abramovitch, R. A. *Can. J. Chem.* **1959**, *37*, 361.
(10) Eigen, M.; Ilgenfritz, G.; Kruse, W. *Chem. Ber.* **1965**, *98*, 1623.
(11) Billman, J. H.; Sojka, S. A.; Taylor, P. R. *J. Chem. Soc., Perkin Trans. 2* **1972**, 2034.

10.1021/jo8027054 CCC: $40.75
Published on Web 02/20/2009

of the ether oxygens to produce dimedone reduces the acidity by 4 orders of magnitude. At the same time, dimedone prefers the chair conformation, and is significantly enolized in solution.[7]

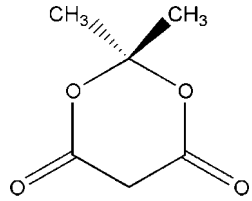

MA

MA has found widespread applications in synthetic chemistry. It has been used as a reactant in the synthesis and design of a vast range of organic compounds having utility in the context of drugs and pharmaceuticals.[12,13] It has also been used as a mild acid catalyst in aqueous solution, the consequent conjugate base stabilized by electron delocalization over the two carbonyl groups being readily formed.[14] The enolate anion can also function as a nucleophile in many condensation reactions, for example, the Knoevenagel reaction. MA can also act as an electrophile due to the presence of two carbonyl groups. Given its chemical versatility, this compound finds applications in the field of Divergent-Oriented Synthesis and in Multi-Component Reactions.[15] Thus, it has been utilized in various realms of synthetic organic chemistry, and has been extensively employed for the development of combinatorial libraries of organic molecules of both skeletal and fragmental diversity. In addition, this compound and its derivatives have found applications as important synthetic intermediates and valuable reagents in the design and synthesis of complex organic compounds such as natural products and their analogues. The chemical versatility of MA has been summarized in two review articles.[16,17]

Detailed theoretical investigations on the structure and origin of the acidity in MA have primarily focused on stabilizing or destabilizing interactions which are specific to MA and its conjugate base.[18] One such analysis by Arnett and Harrelson mentions restricted rotation about the ester linkage to be a cause of the high C−H acidity in MA.[7] Byun et al.[19] describe the importance of the structure and stability of the enolate anion on the acidity. Recently Nakamura et al.,[8] using the reactive hybrid orbital (RHO) theory, have proposed that the energy levels of the unoccupied RHOs of the C−H moiety of MA interact with the unoccupied orbitals of the adjacent carbonyl groups thus facilitating electron acceptance by the C−H moiety.

In view of the diverse applications of this molecule in synthetic chemistry, the continuing discussion of its acidity, and the origin of the boat conformation, we have undertaken an experimental electron density determination for crystalline MA to address these questions. We present the salient features associated with chemical bonding along with the topological characterization of the electron density, including all the intra- and intermolecular bond critical points using the quantum theory of atoms in molecules (QTAIM).[20] Such studies also allow the estimation of atomic charges, in particular for the acidic methylene hydrogen atoms, the electrostatic potential on the molecular surface, and evaluation of the energetics associated with C−H···O intermolecular hydrogen bonds, as well as the characterization of dipolar C···O contacts.

2. Experimental Section

a. Strategy of Data Collection and Reduction. Colorless, clean crystals of MA were grown by slow evaporation from acetone. One such crystal (dimensions 0.3 mm × 0.3 mm × 0.1 mm) was mounted with oil inside a nylon loop. It was cooled to 20.00(5) K with use of an open flow helium cryostat.[21−23] X-ray diffraction measurements were performed with a Rigaku R-axis Rapid diffractometer, equipped with a high-power Mo rotating anode generator (18 kW), graphite monochromator, and curved image plate detector, and using Mo Kα radiation.

To obtain quality data having sufficiently high resolution and redundancy, 12 different runs (divided into 6 pairs) ranging from 0 to 180° in ω were collected at different χ and φ settings. A 4° ω-scan range was taken to avoid significant overlap of reflections in any given image. For each pair of runs, a 2° shift in start angle provided a half-oscillation range overlap for precise scaling and avoided the use of partial reflections. A frame time of 140 s was chosen to maximize the intensity of the Bragg reflections and also to avoid saturation of the strongest reflections. The entire experiment was completed in about two days.

The reflections were indexed with HKL2000,[24] and the collected data were integrated by using the VIIPP data integration program[25,26] based on the reflection positions predicted from HKL2000. The program SORTAV[27] was used for scaling and averaging of reflections in the *mmm* point group. Absorption was considered negligible ($\mu = 0.13$ mm^{-1}). Data reduction statistics can be found in Table 1.

b. Crystal Structure Determination: Spherical and Multipole Refinements. The crystal structure of MA was resolved by using direct methods and a least-squares independent atom refinement

TABLE 1. Crystal Structure Information and Experimental Details on Meldrum's Acid

formula	$C_8H_{12}O_4$
formula weight	144.12
crystal system	orthorhombic
space group	*Pbca*
a (Å)	5.9053(1)
b (Å)	13. 5525(2)
c (Å)	16. 3577(3)
vol (Å^3), Z	1309.1(1), 8
T (K)	20.00(5)
λ (Å)	0.71073
$(\sin\theta/\lambda)_{max}$ (Å^{-1}) or d_{max} (Å)	1.322, 0.380
total no. of parameters	451
collected reflections	172179
unique reflections	10626
no. included in the refinement ($I > 3\sigma(I)$)	8565
data completeness (all data, $d > 0.5$ Å)	84%, 94.5%
average redundancy	16.1
R_{int} (all, $I > 3\sigma(I)$)	0.0227, 0.0213
R_1(spherical), wR_2 (spherical)	0.0232, 0.0760
$R(F)$ (multipole), $wR(F)$ (multipole)	0.0126, 0.0119
GOF	1.0473

(12) Song, A.; Wang, X.; Lam, K. S. *Tetrahedron Lett.* **2003**, *44*, 1755.
(13) Tang, J.; Wu, L. L.; Huang, X. *Chin. Chem. Lett.* **2003**, *14*, 661.
(14) Wang, S.-Y.; Ji, S.-J.; Su, X.-M. *Chin. J. Chem.* **2008**, *26*, 22.
(15) Gerencser, J.; Dorman, G.; Darvas, F. *QSAR Comb. Sci.* **2006**, *25*, 439.
(16) McNab, H. *Chem. Soc. Rev.* **1978**, *7*, 345.
(17) Ivanov, A. S. *Chem. Soc. Rev.* **2008**, *37*, 789.
(18) Lee, I.; Han, I. S.; Kim, C. K.; Lee, H. W. *Bull. Korean Chem. Soc.* **2003**, *24*, 1141.
(19) Byun, K.; Mo, Y.; Gao, J. *J. Am. Chem. Soc.* **2001**, *123*, 3974.
(20) Bader, R. F. W. *Atoms in Molecules: A Quantum Theory*, The International Series of Monographs of Chemistry; Halpern, J., Green, M. L. H., Eds.; Clarendon Press: Oxford, UK, 1990; pp 1−438.
(21) Hardie, M. J.; Kirschbaum, K.; Martin, A.; Pinkerton, A. A. *J. Appl. Crystallogr.* **1998**, *31*, 815.
(22) Kirschbaum, K.; Martin, A.; Parrish, D.; Pinkerton, A. A. *J. Phys.: Condens. Matter* **1999**, *11*, 4483.
(23) Ribaud, L.; Wu, G.; Zhang, Y.; Coppens, P. *J. Appl. Crystallogr.* **2001**, *34*, 76.

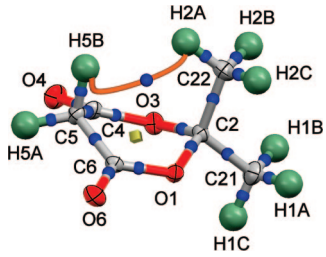

FIGURE 1. ORTEP drawing of Meldrum's acid at 20 K showing atomic thermal ellipsoids at the 90% probability level for non-hydrogen atoms (hydrogen atoms are drawn with arbitrary radii) and the atom numbering scheme. The bond path for the H(5B)···H(2A) intramolecular interaction (orange in color) obtained from the experimental data is also shown. The blue balls indicate (3,−1) bond critical points, and the yellow cube indicates a (3,+1) ring critical point. The programs Mercury[37] and WinXPRO[33,34] were used.

was carried out with SHELXTL.[28] All the non-hydrogen atoms were refined with anisotropic displacement parameters. The hydrogen atoms in the molecule were located from a Fourier difference map and refined with isotropic displacement parameters. Refinement statistics for this spherical atom refinement can be found in Table 1. This model served as the starting point for the aspherical atom refinement, using the Hansen−Coppens multipole formalism[29] as implemented in the XD program.[30] The Volkov and Macchi data bank using STO atomic relativistic wave functions obtained at the PBE/QZ4P level of theory for neutral atoms in ground state configurations was used. Only reflections with intensities above $3\sigma(I)$ were retained in the refinement. The multipole population parameters for all the oxygen and carbon atoms were refined up to the hexadecapole level and the hydrogen atoms up to the quadrupole level. Chemical constraints were initially imposed on carbonyl oxygens, ether oxygens, methyl hydrogens, and methylene hydrogens. These constraints were released slowly and progressively during the later stages of refinement. The final model was refined unconstrained. The condition of electroneutrality was imposed on the whole molecule for all the refinement cycles.

The expansion and contraction parameters (κ' and κ'') were assigned depending on the atom type, chemical hybridization, and electronic environment. Seven κ sets (one for the carbonyl oxygens, one for the ether oxygens, one for the carbonyl carbons, one each for the flagpole carbons, and one for the methyl carbons) were implemented in the refinement. The κ' and κ'' parameters for the hydrogen atoms were fixed to 1.2 during the refinement. Initially, only the atomic coordinates and thermal displacement parameters for the non-hydrogen atoms were refined by using all data ($0.0 \leq \sin\theta/\lambda \leq 1.32$ Å^{-1}), whereas those for the hydrogens were refined by using low-angle data ($\sin\theta/\lambda \leq 1.00$ Å^{-1}). The C−H and O−H distances were extended to the neutron bond lengths ($C_{methylene}H$ = 1.092 Å; $C_{methyl}H$ = 1.059 Å).[31] In the early stages of the refinement, the monopole populations and the expansion/contraction parameters κ'' were refined together, followed by refinement of multipoles and κ' in separate groups. Thus, highly correlated parameters were initially refined in separate groups. The refinements were stable and full convergence of all parameters was attained during the refinement. In the final refinement cycle, all the parameters were refined together and full convergence to a final residual of 0.0126 was achieved.

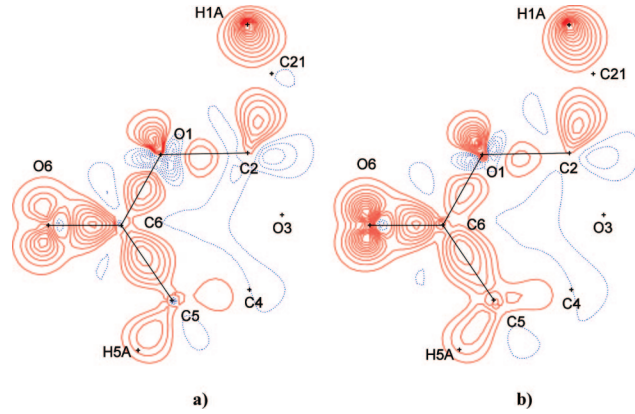

FIGURE 2. Static multipole deformation density map in the O(6)−C(6)−O(1) plane: (a) experimental and (b) theoretical solid state calculations. Contour intervals are drawn at 0.1 eÅ^{-3}. Red solid lines are positive contours and blue dotted lines are negative contours.

c. Evaluation of Data Quality. A number of parameters from different tests were used to demonstrate the quality of the data, and the adequacy of the refinement (Table 1). The averaged (in 0.05 Å^{-1} intervals) ratios of the observed and calculated structure factors were very close to unity (≤0.6% deviation up to $\sin\theta/\lambda$ = 1.322 Å^{-1}) based on F indicating an accurate scale factor for all data, as well as a good fit for the experimental electron density model over the whole resolution range. The residual electron density (the difference between observed and calculated multipole electron densities) was in the range 0.18/−0.12 eÅ^{-3}, and a residual density map has been deposited (Supporting Information). After the multipole refinement, a further test for the reasonableness of the final model was performed by calculating the total electron density, which was found to be non-negative in all regions of space. Finally, the rigid-bond test[32] demonstrated that the differences of mean-square displacement amplitudes along the interatomic vectors were less than 5×10^{-4} Å^2 suggesting clean deconvolution of the aspherical atomic electron density from the atomic displacement parameters. For the topological characterization of one-electron properties the program packages XDPROP[30] and WinXPRO[33,34] were used.

d. Theoretical Calculations. To complement the experimental results, a density functional theory B3LYP periodic calculation using the 6-311G(d,p) basis set with the experimentally observed molecular geometry was performed with use of the program CRYSTAL98.[35] Theoretical structure factors have been calculated for all possible hkl indices up to $\sin\theta/\lambda$ = 1.3 Å^{-1}, and used for refinements following a similar strategy as that used for the experimental data. A final $R(F)$ = 0.0049 was reached, and the residual electron density showed no peaks above or below 0.14/−0.11 eÅ^{-3}.

3. Results

The results have been summarized as follows. A deformation electron density map is presented in Figure 2. The properties of the bonding critical points of all the covalent bonds are

(24) Otwinowski, Z.; Minor, W. *Methods Enzymol.* **1997**, *276A*, 307.
(25) Zhurov, V. V.; Zhurova, E. A.; Chen, Y.-S.; Pinkerton, A. A. *J. Appl. Crystallogr.* **2005**, *38*, 827.
(26) Zhurova, E. A.; Zhurov, V. V.; Tanaka, K. *Acta Crystallogr.* **1999**, *B55*, 917.
(27) Blessing, R. H. *Cryst. Rev.* **1987**, *1*, 3.
(28) Sheldrick, G. M. *SHELXTL*, Vers.6.14, An Integrated System for Solving, Refining and Displaying Crystal Structures from Diffraction Data; University of Göttingen: Göttingen, Germany, 2000.
(29) Hansen, N.; Coppens, P. *Acta Crystallogr.* **1978**, *A34*, 909.
(30) Volkov, A.; Macchi, P.; Farrugia, L. J.; Gatti, C.; Mallinson, P.; Richter, T.; Koritsanszky, T. *XD2006*, A Computer Program Package for Multipole Refinement and Topological Analysis of Charge Densities and evaluation of intermolecular interaction energies from experimental and theoretical structure factors, 2006.
(31) Allen, F. H.; Kennard, O.; Watson, D. G.; Brammer, L.; Orpen, A. G.; Taylor, R. *J. Chem. Soc., Perkin Trans. 2* **1987**, S1.
(32) Hirshfeld, F. L. *Acta Crystallogr.* **1976**, *A32*, 239.
(33) Stash, A. I.; Tsirelson, V. G. *J. Appl. Crystallogr.* **2002**, *35*, 371.
(34) Stash, A. I.; Tsirelson, V. G. *Crystallogr. Rep.* **2005**, *50*, 202.
(35) Saunders, V. R.; Dovesi, R.; Roetti, C.; Causa, M.; Harrison, N. M.; Orlando, R.; Sicovich-Wilson, C. M. *CRYSTAL98 User's Manual*; University of Torino: Torino, Italy, 1998.

TABLE 2. Bond Critical Points in the Meldrum's Acid Crystal: Intramolecular Bonds[a]

bond	ρ, eÅ^{-3}	$\nabla^2\rho$, eÅ^{-5}	R_{ij}, Å	d_1, Å	d_2, Å	λ_1, eÅ^{-5}	λ_2, eÅ^{-5}	λ_3, eÅ^{-5}	ε	n_{topo}
O(6)−C(6)	2.915	−24.12	1.208	0.789	0.419	−29.019	−26.416	31.317	0.099	1.390
	2.930	−26.41	1.208	0.777	0.431	−26.508	−24.965	25.066	0.062	1.553
O(4)−C(4)	2.986	−24.65	1.202	0.786	0.416	−29.961	−27.793	33.107	0.078	1.409
	2.961	−25.25	1.202	0.775	0.427	−26.931	−25.753	27.431	0.046	1.544
O(1)−C(6)	2.175	−26.96	1.341	0.855	0.487	−19.337	−17.514	9.895	0.104	1.085
	2.112	−18.70	1.341	0.816	0.525	−16.610	−15.923	13.834	0.043	1.076
O(1) - C(2)	1.692	−15.05	1.445	0.868	0.578	−13.355	−12.192	10.502	0.095	0.746
	1.660	−9.29	1.445	0.845	0.602	−12.627	−11.561	14.897	0.092	0.702
O(3)−C(4)	2.148	−26.55	1.352	0.849	0.504	−18.685	−17.295	9.430	0.080	1.076
	2.057	−17.01	1.352	0.817	0.536	−16.183	−15.159	14.333	0.068	1.031
O(3)−C(2)	1.746	−15.70	1.440	0.861	0.580	−13.903	−12.791	10.997	0.087	0.782
	1.686	−9.68	1.440	0.842	0.599	−12.863	−11.716	14.899	0.098	0.725
C(4)−C(5)	1.776	−14.50	1.504	0.790	0.715	−12.526	−11.745	9.773	0.066	1.021
	1.731	−11.79	1.504	0.789	0.716	−11.796	−11.199	11.210	0.053	0.863
C(6)−C(5)	1.758	−14.52	1.502	0.791	0.711	−12.404	−11.608	9.496	0.069	1.017
	1.743	−12.21	1.502	0.789	0.713	−11.985	−11.343	11.123	0.057	0.884
C(2)−C(21)	1.804	−15.86	1.511	0.821	0.690	−12.820	−12.412	9.372	0.033	1.084
	1.760	−13.43	1.511	0.816	0.695	−12.304	−11.852	10.725	0.038	0.933
C(2)−C(22)	1.759	−14.44	1.519	0.814	0.705	−12.159	−11.969	9.686	0.016	1.005
	1.705	−11.94	1.519	0.815	0.704	−11.665	−11.202	10.924	0.041	0.850
C(5)−H(5A)	1.891	−21.16	1.092	0.696	0.396	−17.875	−16.844	13.563	0.061	0.968
	1.841	−18.30	1.092	0.710	0.382	−17.203	−16.845	15.743	0.021	0.979
C(5)−H(5B)	1.821	−18.91	1.092	0.704	0.388	−16.698	−16.272	14.064	0.026	0.965
	1.832	−19.13	1.092	0.709	0.383	−17.112	−16.891	14.874	0.013	0.952
C(21)−H(1A)	1.880	−19.01	1.059	0.648	0.411	−16.662	−16.004	13.657	0.041	1.040
	1.964	−20.68	1.059	0.677	0.382	−18.336	−18.125	15.777	0.012	1.028
C(21)−H(1B)	1.835	−17.15	1.059	0.651	0.408	−16.039	−15.275	14.161	0.050	1.051
	1.966	−20.58	1.059	0.678	0.381	−18.260	−18.200	15.881	0.003	1.037
C(21)−H(1C)	1.847	−18.22	1.059	0.655	0.404	−16.585	−15.681	14.049	0.058	1.025
	1.965	−20.52	1.059	0.673	0.386	−18.298	−17.939	15.717	0.020	1.033
C(22)−H(2A)	1.901	−19.70	1.059	0.647	0.412	−16.966	−16.144	13.410	0.051	1.042
	1.968	−21.27	1.059	0.677	0.382	−18.424	−18.339	15.490	0.005	1.026
C(22)−H(2B)	1.834	−17.08	1.059	0.655	0.404	−16.264	−15.189	14.371	0.071	1.049
	1.963	−20.77	1.059	0.677	0.382	−18.372	−18.083	15.689	0.016	1.022
C(22)−H(2C)	1.852	−17.70	1.059	0.641	0.418	−16.213	−15.090	13.604	0.074	1.061
	1.952	−20.56	1.059	0.675	0.384	−18.153	−18.045	15.642	0.006	1.015

[a] First line: experiment. Second line: theoretical calculation. ρ is the electron density; $\nabla^2\rho$ is the Laplacian; R_{ij} is the interatomic distance, d_1 and d_2 are the distances from the critical point to atoms 1 and 2; λ_1, λ_2, and λ_3 are the principal curvatures, ε is the bond ellipticity, and n_{topo} is the topological bond order.[40]

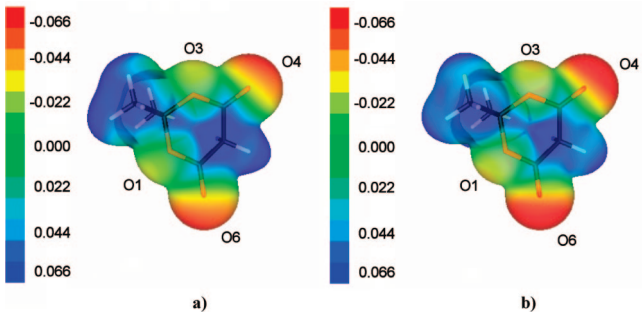

FIGURE 3. A view of the electrostatic potential (prepared with gOpenMol[50,51]) mapped onto the molecular surface (0.001au = 0.00675 eÅ^{-3}) obtained from (a) experiment and (b) solid state theory calculations. The color scheme ranges from red (−0.066 eÅ^{-1}) via green (0.0 eÅ^{-1}) to blue (+0.066 eÅ^{-1}).

reported in Table 2, and a corresponding graphical representation is superimposed on an ORTEP plot of the molecule in Figure 1. The atomic charges obtained from integration over the atomic basins as defined by the zero flux surfaces, along with the corresponding atomic volumes, are listed in Table 3. The derived electrostatic potential projected onto the molecular surface is represented in Figure 3. The properties of all the closed shell interactions are presented in Table 4, with graphical examples shown in Figures 4 and 6, and their impact on the molecular packing is shown in Figure 5.

TABLE 3. Atomic Charges (q) and Volumes (Ω) Integrated over the Atomic Basins in Meldrum's Acid[a]

atom	$q(\Omega)_{AIM}$ (e$^-$)	Ω_{AIM} (Å^3)	atom	$q(\Omega)_{AIM}$ (e$^-$)	Ω_{AIM} (Å^3)
O1	−1.067	13.739	C22	0.304	9.187
	−0.913	13.612		0.105	9.211
O3	−1.037	13.999	H5A	0.105	6.904
	−0.906	13.911		0.071	7.964
O6	−1.196	17.474	H5B	0.105	5.455
	−1.092	17.248		0.134	5.538
O4	−1.183	19.439	H1A	−0.054	7.725
	−1.096	19.089		0.032	7.507
C6	1.593	4.608	H1B	−0.047	7.267
	1.343	5.017		0.036	7.104
C4	1.565	4.877	H1C	−0.043	8.078
	1.341	5.268		0.007	7.915
C2	0.734	4.938	H2A	−0.039	6.459
	0.652	4.947		0.047	6.457
C5	0.052	8.606	H2B	−0.048	7.967
	0.063	8.100		0.041	7.716
C21	0.336	8.841	H2C	−0.068	7.866
	0.105	8.706		0.027	8.058
$\sum_{experiment}$				0.008	163.428
$\sum_{theory}$				0.001	163.371

[a] $q(\Omega)$ and $V(\Omega)$ are atomic charges and volumes integrated over atomic basins, L_{err} = 0.0004 au (both experiment and theory); $L_{err} = (\sum L_\Omega^2/N_{atoms})^{1/2}$, where L_Ω is the atomic integrated Lagrangian; unit cell volume/8 = 163.75 Å^3.

TABLE 4. Bond Critical Points in the Meldrum's Acid Crystal: Closed-Shell Interactions[a]

bond	ρ, eÅ^{-3}	$\nabla^2\rho$, eÅ^{-5}	R_{ij}, Å	d_1, Å	d_2, Å	λ_1, eÅ^{-5}	λ_2, eÅ^{-5}	λ_3, eÅ^{-5}	g	v	h_e	D_e
O(4)···H(5B)	0.076	1.26	2.322	0.966	1.383	−0.248	−0.165	1.678	0.0103	−0.0076	0.0027	9.98
$x - {}^1/_2, -y + {}^1/_2, -z$	0.078	1.19	2.322	0.948	1.379	−0.277	−0.200	1.644	0.0116	−0.0075	0.0024	9.85
O(6)···C(6)	0.082	0.85	2.905	1.473	1.449	−0.222	−0.041	1.117	0.0077	−0.0066	0.0011	8.66
$x + {}^1/_2, +y, -z + {}^1/_2$	0.075	0.81	2.905	1.468	1.436	−0.247	−0.051	1.104	0.0072	−0.0059	0.0012	7.75
H(2A)···H(5B)	0.067	0.82	2.201	1.112	1.234	−0.193	−0.094	1.102	0.0069	−0.0054	0.0015	7.09
x, y, z	0.056	0.79	2.201	1.170	1.100	−0.205	−0.120	1.119	0.0065	−0.0047	0.0018	6.17
O(6)···H(1A)	0.040	0.66	2.684	1.530	1.193	−0.107	−0.080	0.842	0.0051	−0.0034	0.0017	4.46
$-x, +y + {}^1/_2, -z + {}^1/_2$	0.046	0.63	2.684	1.502	1.191	−0.149	−0.120	0.900	0.0051	−0.0036	0.0015	4.73
O(4)···H(2A)	0.035	0.44	2.740	1.584	1.157	−0.077	−0.064	0.584	0.0035	−0.0024	0.0011	3.15
$x - {}^1/_2, -y + {}^1/_2, -z$	0.036	0.42	2.740	1.581	1.165	−0.091	−0.077	0.591	0.0034	−0.0024	0.0009	3.15
O(3)···H(1B)	0.029	0.41	2.817	1.187	1.641	−0.066	−0.059	0.531	0.0031	−0.0021	0.0010	2.76
$-x, -y, -z$	0.028	0.38	2.817	1.174	1.644	−0.081	−0.055	0.511	0.0029	−0.0019	0.0010	2.49
O(4)···H(1B)	0.019	0.31	2.921	1.713	1.249	−0.043	−0.036	0.391	0.0023	−0.0014	0.0009	1.84
$-x - {}^1/_2, +y - {}^1/_2, +z$	0.022	0.29	2.921	1.679	1.243	−0.058	−0.043	0.393	0.0022	−0.0014	0.0008	1.84
O(4)···H(2A)	0.023	0.30	2.947	1.729	1.245	−0.052	−0.038	0.388	0.0023	−0.0015	0.0008	1.97
$x - 1, +y, +z$	0.021	0.27	2.947	1.716	1.236	−0.053	−0.042	0.361	0.0020	−0.0013	0.0007	1.71
O(1)···H(1C)	0.019	0.23	3.083	1.753	1.350	−0.035	−0.024	0.287	0.0017	−0.0011	0.0006	1.44
$x + {}^1/_2, +y, -z + {}^1/_2$	0.017	0.21	3.083	1.765	1.318	−0.037	−0.023	0.269	0.0016	−0.0010	0.0006	1.31
H(5A)···H(1C)	0.025	0.29	2.489	1.241	1.241	−0.081	−0.052	0.418	0.0022	−0.0015	0.0007	1.97
$-x - {}^1/_2, +y + {}^1/_2, +z$	0.027	0.30	2.489	1.220	1.281	−0.089	−0.068	0.452	0.0023	−0.0016	0.0007	2.10
H(5B)···H(1A)	0.028	0.40	2.550	1.281	1.285	−0.071	−0.035	0.504	0.0031	−0.0020	0.0011	2.63
$-x + {}^1/_2, +y + {}^1/_2, +z$	0.022	0.38	2.550	1.269	1.284	−0.060	−0.042	0.484	0.0029	−0.0017	0.0012	2.23

[a] First line: experiment. Second line: solid state theoretical calculation. ρ is the electron density; $\nabla^2\rho$ is the Laplacian; R_{ij} is the interatomic distance, d_1 and d_2 are the distances from the critical point to atoms 1 and 2; λ_1, λ_2, and λ_3 are the principal curvatures; g, v, and h_e are the kinetic, potential, and total electronic energies at the critical point (in au), respectively. D_e is an approximate dissociation energy calculated as $D_e = -v/2$ (in kJ/mol).[60] All bond paths and virial paths have been verified.

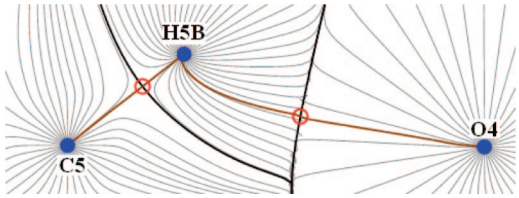

FIGURE 4. The electron density gradient map showing the H(5B)···O(4) intermolecular hydrogen bond obtained from experimental data. The red open circles indicate (3,−1) bond critical points and blue full circles are (3,−3) critical points. The bond path is shown in brown.

4. Discussion

a. Structural Analysis. An ORTEP plot of MA showing the atom numbering is shown in Figure 1. The general structure parameters are in good agreement with the previous report.[3] The boat conformation may be defined either by the deviation of C(2) and C(5) from the C(4), C(6), O(1), O(3) plane (0.4815(2) and 0.3956(2) Å, respectively), or by the Cremer and Pople ring-puckering parameters[36] for the six-membered ring (Q = 0.5084(2) Å, θ = 86.10(2)°, ϕ = 61.474(19)°, respectively). The geometry of the lactone groups again suggests conjugation of the ether oxygens (C(6)−O(1) and C(4)−O(3) are 1.3424(3) and 1.3527(3) Å, respectively). This will be discussed in greater detail below.

b. Intramolecular Interactions: Topological Analysis of the Total Electron Density. Figure 2 represents the static deformation density (the difference between the total electron density and a superposition of spherical atoms) obtained from both experiment and theory (in the O(6)−C(6)−O(1) plane), thereby giving a qualitative picture of the covalent bonds present in the molecule along with the lone pairs on the carbonyl

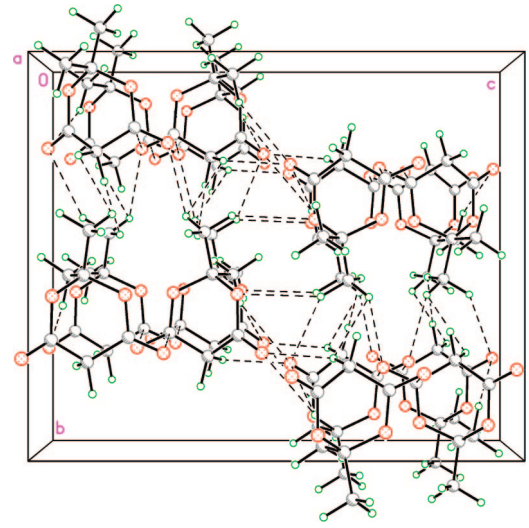

FIGURE 5. Packing diagram depicting C═O···C═O contacts and C−H···O hydrogen bonding interactions for which corresponding bond paths and critical points have been identified. The distances for the antiparallel motif d(C6···O6) = 2.9047(6) Å and 3.0864(7) Å, respectively. For the perpendicular motif, d(C4···O4) = 3.0047(5) Å.

(36) Cremer, D.; Pople, J. A. *J. Am. Chem. Soc.* **1975**, *97*, 1354.

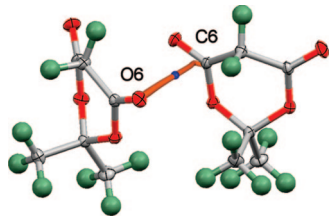

FIGURE 6. Bond path depiction for the dipolar C(6)···O(6) intermolecular contact in the crystalline lattice obtained from experiment. The brown thick line shows the bond path trajectory and the blue ball indicates the (3,−1) bond critical point.

oxygen. A more quantitative picture is obtained from a topological analysis of the total electron density, in particular the properties of the saddle points associated with the covalent bonds. Table 2 lists all the intramolecular (3,−1) bond critical points obtained from both experiment and theory in the MA crystal. Good agreement (within a few hundredths eÅ^{-3}) is observed between the electron density values obtained from both experiment and theory.

However, in the case of the Laplacian of the electron density the agreement is less satisfactory, primarily due to the differences in λ_3 values, this feature being related to the known deficiency in the multipole model formalism of the electron density.[38,39] As expected, the shortest, strongest bonds have the highest values of the electron density accumulation at the critical points. To put this on a more quantitative basis, their topological bond orders[40−42] have been calculated from the principal electron-density curvatures (λ_1, λ_2, λ_3) and electron-density values (ρ) (Table 2) by using the equation $n_{\text{topo}} = a + b\lambda_3 + c(\lambda_1 + \lambda_2) + d\rho_{\text{CP}}$ (all values in atomic units) for all the covalent bonds. Coefficients a, b, c, and d are defined as reported by Tsirelson et al.[40] Thus, the bonds of the carbonyl groups with higher electron density values (2.915−2.986 eÅ^{-3}) at the critical points, followed by the C(sp^2)−O (2.175−2.148 eÅ^{-3}) and then C(sp^3)−O (1.692−1.746 eÅ^{-3}) bonds correlate strongly with the topological bond orders of 1.390−1.409 for carbonyl groups, 1.076−1.085 for C(sp^2)−O(ether oxygen) and 0.746−0.782 for C(sp^3)−O(ether oxygen). It is also of interest to note that the two C(sp^3)−O bonds have the lowest bond order values, thereby indicating that in a chemical reaction involving this molecule these are most susceptible to rupture.

c. Atomic Charges. Sites of electrophilic or nucleophilic attack, acidic hydrogen atoms, and potential hydrogen bond donor/acceptor atoms may be predicted from atomic charges. Atomic charges were determined by integration over the atomic basins delimited by zero flux surfaces as defined in Bader's QTAIM theory,[20] and they are reported in Table 3 for both the experimental data and the solid-state theoretical calculation. Table 3 also lists the volumes of the atomic basins. The accuracy of the performed integrations is confirmed by the integrated Lagrangian being reasonably small (0.0004 au), the sum of the atomic charges having very small values (the molecule should be neutral), and the sums of the atomic volumes reproducing the unit cell volume per molecule with an error of 0.2%.

It is of interest to note that, whereas hydrogen atoms bound to sp^3-hybridized carbon (e.g., $H_{1a,b,c}$, $H_{2a,b,c}$) typically carry zero or slightly negative charges, the two methylene hydrogens in MA are acidic, their charges being 0.105 e$^-$ (from experiment), and 0.071 and 0.134 e$^-$ (from theory), respectively. However, they carry significantly less charge than typical weakly acidic OH groups, for example, the experimental charges on hydrogen for the OH groups in a series of estrogens range from 0.54 to 0.62 e$^-$.[43−46] Thus, the most important contribution to the acidity of MA is not the charge distribution in the parent acid, but rather the stabilization due to the extensive conjugation in the resulting enolate anion, where C(5) and the remaining hydrogen atom become coplanar with the two lactone groups.[47] Although the experimental charges for the two methylene hydrogens are the same, theory assigns a slightly higher positive charge to H(5B). This hydrogen is also the farthest out of the plane of the putative enolate anion, suggesting that deprotonation involves H(5B) rather than H(5A). The carbon atoms C(4) and C(6) have high positive charges (1.565 and 1.593 e$^-$, respectively) thereby proving their susceptibility to nucleophilic attack. All oxygens carry significant negative charges; however, most electrophilic reactions involve the enolate anion rather than the neutral acid.

d. Electrostatic Potential of Meldrum's Acid. A useful measure of the direction of nucleophilic or electrophilic attack, as well as the propensity to form hydrogen bonds, may be obtained from the electrostatic potential (ESP), which can be derived from the charge distribution.[48] The ESP maps projected onto the molecular surface (defined as the electron density isosurface of 0.001au[49]) for a single molecule taken from the crystal, as determined from experiment and theory, are shown in Figure 3. The experimental and theoretical results are in excellent agreement. The most negative regions are in the vicinity of the carbonyl oxygens, being more electronegative than the ether oxygens of the lactone groups.

As shown below, the strongly negative potentials are responsible for the formation of hydrogen bonds. The methylene hydrogens are associated with a region of positive electrostatic potential, these being prone to undergo abstraction by a base, and also attracted to negative areas around the oxygen atom in hydrogen bond formation.

e. Boat Conformation. Dipole moment measurements[4,5] and NMR studies[52] on MA show that the boat conformation of the six-membered ring is preferred. However, there has been a long-standing debate concerning the energetics which stabilize this conformation. The experimental dipole moment estimated from

(37) Macrae, C. F.; Bruno, I. J.; Chisholm, J. A.; Edgington, P. R.; McCabe, P.; Pidcock, E.; Rodriguez-Monge, L.; Taylor, R.; van de Streek, J.; Wood, P. A. *J. Appl. Crystallogr.* **2008**, *41*, 466.
(38) Volkov, A.; Abramov, Yu.; Coppens, P.; Gatti, C. *Acta Crystallogr.* **2000**, *A56*, 332.
(39) Tsirelson, V. G.; Stash, A. I.; Potemkin, V. A.; Rykounov, A. A.; Shutalev, A. D.; Zhurova, E. A.; Zhurov, V. V.; Pinkerton, A. A.; Gurskaya, G. V.; Zavodnik, V. E. *Acta Crystallogr.* **2006**, *B62*, 676.
(40) Tsirelson, V. G.; Bartashevich, E. V.; Stash, A. I.; Potemkin, V. A. *Acta Crystallogr.* **2007**, *B63*, 142.
(41) Zhurova, E. A.; Stash, A. I.; Tsirelson, V. G.; Zhurov, V. V.; Bartashevich, E. V.; Potemkin, V. A.; Pinkerton, A. A. *J. Am. Chem. Soc.* **2006**, *128*, 14728.
(42) Howard, S. T.; Lamarche, O. *J. Phys. Org. Chem.* **2003**, *16*, 133.
(43) Yearley, E. J.; Zhurova, E. A.; Zhurov, V. V.; Pinkerton, A. A. *J. Am. Chem. Soc.* **2007**, *129*, 15013.
(44) Zhurova, E. A.; Matta, C. F.; Wu, N.; Zhurov, V. V.; Pinkerton, A. A. *J. Am. Chem. Soc.* **2006**, *128*, 8849.
(45) Parrish, D.; Zhurova, E. A.; Kirschbaum, K.; Pinkerton, A. A. *J. Phys. Chem. B* **2006**, *110*, 26442.
(46) Yearley, E. J.; Zhurova, E. A.; Zhurov, V. V.; Pinkerton, A. A. *J. Mol. Struct.* **2008**, *890*, 240.
(47) Kuhn, N.; Al-Sheikh, A.; Steimann, M. *Z. Naturforsch. B* **2003**, *58*, 481.
(48) Su, Z.; Coppens, P. *Acta Crystallogr.* **1992**, *A48*, 188.
(49) Bader, R. F. W.; Carroll, M. T.; Cheeseman, J. R.; Chang, C. *J. Am. Chem. Soc.* **1987**, *109*, 7968–7979.
(50) Bergman, D. L.; Laaksonen, L.; Laaksonen, A. *Mol. Graph. Model.* **1997**, *15*, 301.
(51) Laaksonen, L. *J. Mol. Graph.* **1992**, *10*, 33.
(52) Ayras, P.; Partanen, A. *Finn. Chem. Lett.* **1976**, 110.

the electron density analysis in MA is 4.60 D, which is slightly higher than the dipole moment of 3.18 D measured in dioxan.[5] It is still not clear why MA prefers to have a boat conformation. Lee et al.[18] suggest that the planarity of the lactone ring imposes significant constraints due to n → π^* interactions which may require the conformation to be boat. In addition, they find that the charges on the two out-of-plane carbon atoms are of opposite sign and thus electrostatic attraction would provide additional stability for the boat conformation. In contrast, we find that the carbon atom C(5) is close to neutral (+0.052 e^-) thus minimizing any electrostatic interaction with the positively charged carbon atom C(2) (+0.734 e^-).

As shown in Figure 1, an additional important feature in the MA molecule that provides significant stabilization to the boat conformation is the presence of an intramolecular H···H bonding interaction involving hydrogen atoms H(5B) attached to C(5), and H(2A) attached to the methyl carbon C(22). This type of hydrogen−hydrogen bonding interaction has solicited significant interest in recent years.[53,54] In the present case, the distance between the participating hydrogens of 2.201 Å is less than the sum of the van der Waals radii of two hydrogen atoms of 2.4 Å.[55] A (3,−1) critical point in the electron density (Table 4), a bond path and a *virial* path in the (negative) potential energy density field strongly suggest the bonding nature of this interaction.[56] The bonding is characterized by a modestly positive value of the electron density, a positive Laplacian, and positive electronic energy density at the critical point, which are indicators of a closed-shell character for this interaction.[57] From the Espinosa et al. relationship,[60] an estimated local stabilization of ∼7 kJ/mol imparted by this interaction provides significant stabilization of the boat conformation.

We note that the most stable conformers of the equally acidic 5-methyl- and 5-ethyl-MA are predicted to be boat with the 5-H atom in the axial position. Thus the potential for H···H bond formation is again present. In contrast, dimedone is predicted to prefer the chair conformation, which would preclude such an interaction.[8,58,59]

f. Intermolecular Interactions. The crystal packing is predominantly dictated by intermolecular C−H···O, C═O···C═O, and H···H contacts in the solid state. Seven hydrogen bonds of the C−H···O type, one contact of the C···O type, and two H···H interactions, along with the topological properties associated with these interactions (evaluated using both experiment and theory), have been determined for the MA crystal (Table 4). All these interactions have a bond path in the electron density and a *virial path* in the negative potential energy density associated with them, which thus demonstrates the bonding nature of these interactions.[56] The strongest interaction is between O(4), a carbonyl oxygen, and H(5B) as shown in Figure 4.

This interaction, along with the absence of any hydrogen bond involving H(5A), lends additional credence to the above hypothesis that H(5B) is the atom most likely to be abstracted by base. All of the interactions for which bond paths were characterized are indicated in the packing diagram in Figure 5.

The interactions of pairs of dipolar carbonyl groups in the solid state have been previously extensively studied.[61] In MA, the C(6)−O(6) carbonyl groups stack parallel to *a* in a continuous approximately antiparallel ((C(6)···O(6) = 2.9047(6) and 3.0864(7) Å) motif spanning the *a* glide plane. However, only one critical point is observed in the electron density (Figure 6). The other carbonyl group forms a continuous perpendicular motif parallel to *a* ((C(4)···O(4) = 3.0047(5) Å), but again there is no critical point observed in the electron density.

We note (Table 4) that the stabilization provided by each of the three types of intermolecular interactions is of the order of a weak hydrogen bond.

5. Conclusions

This article presents a detailed electron density study of Meldrum's acid, including the analysis of the topological properties of the electron density, and the derived electrostatic potential. The boat conformation of the six-membered ring, the acidity of the methylene hydrogen atoms, and the chemical reactivity have been rationalized in terms of the electron density distribution. In particular, stabilization of the boat conformation by an H···H interaction has been identified for the first time. In addition, the stabilization of the crystal lattice by weak intermolecular interactions has been described.

Acknowledgment. We thank Professor James H. Davis for bringing the interest in Meldrum's acid to our attention, and the College of Arts & Sciences for support of the crystallographic facilities.

Supporting Information Available: Crystallographic information file (CIF), scale factor plot, normal probability plot, residual electron density map, and tables of atomic coordinates, and bond lengths and angles. This material is available free of charge via the Internet at http://pubs.acs.org.

JO8027054

(53) Matta, C. F.; Hernandez-Trujillo, J.; Tang, T.-H.; Bader, R. F. W. *Chem.−Eur. J.* **2003**, *9*, 1940.
(54) Matta, C. F. In *Hydrogen Bonding−New Insight*; Grabowski, S., Ed.; Challenges and Advances in Computational Chemistry and Physics Series; Springer: Dordrecht, The Netherlands, 2006; pp 337−376.
(55) Pauling, L. *The Nature of the Chemical Bond*, 3rd ed.; Cornell University Press: Ithaca, NY, 1960.
(56) Bader, R. W. F. *J. Phys. Chem.* **1998**, *A102*, 7314.
(57) Gatti, C. *Z. Kristallogr.* **2005**, *220*, 399.
(58) Mashima, M.; Matsuoka, M.; Lei, Y. X.; Rappoport, Z. *J. Org. Chem.* **2004**, 5947.
(59) Karni, M.; Bernasconi, C. F.; Rappoport, Z. *J. Org. Chem.* **2008**, 2980.
(60) Espinosa, E.; Molins, E. *J. Chem. Phys.* **2000**, *11*, 5686.
(61) Allen, F. H.; Baalham, C. A.; Lommerse, J. P. M.; Raithby, P. R. *Acta Crystallogr.* **1998**, *B54*, 320.